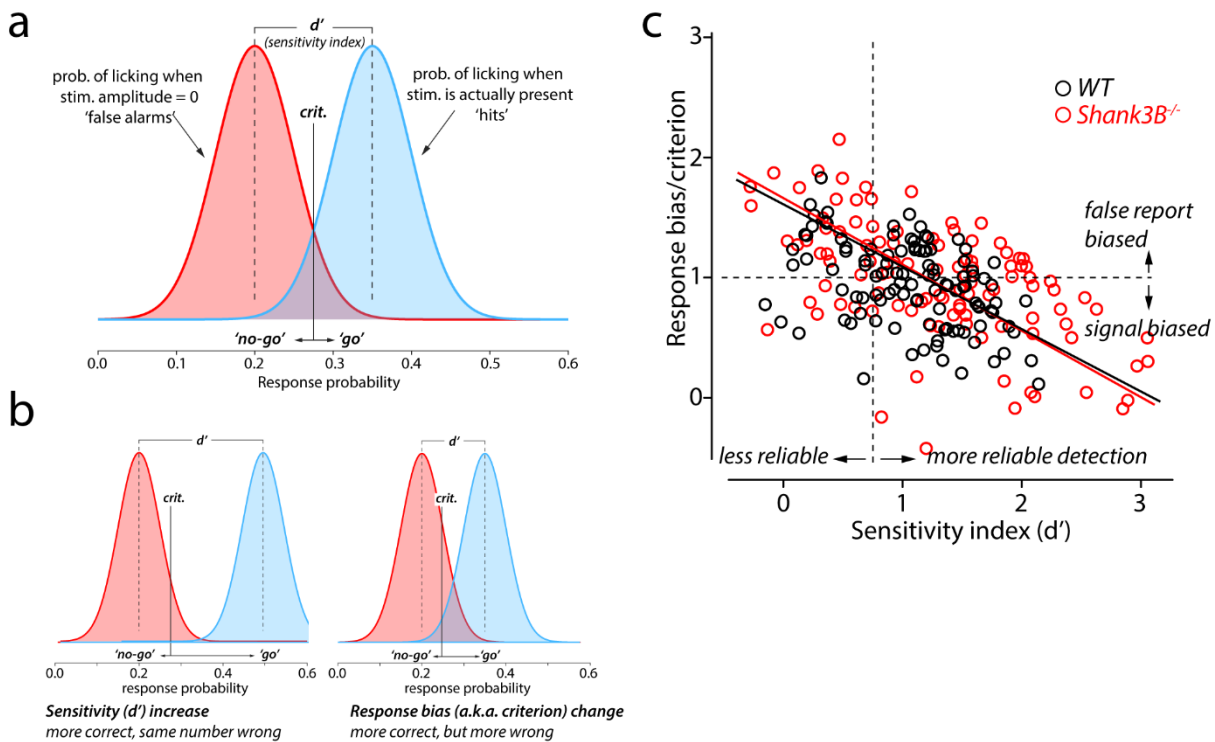
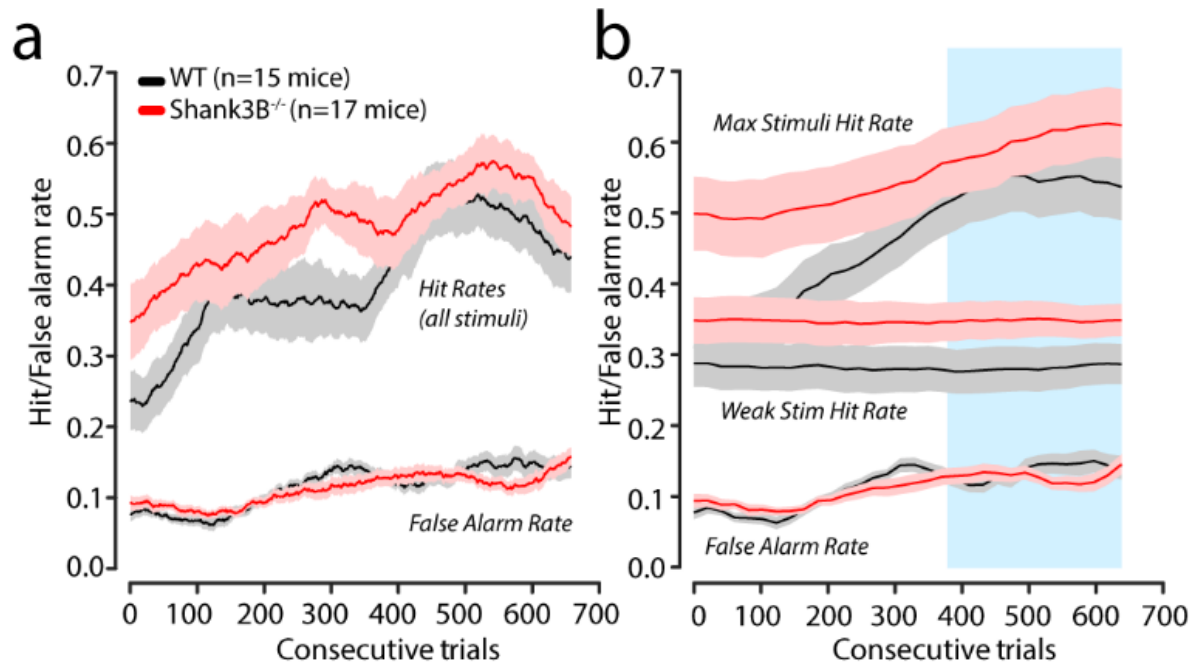


Supplementary Figure 1



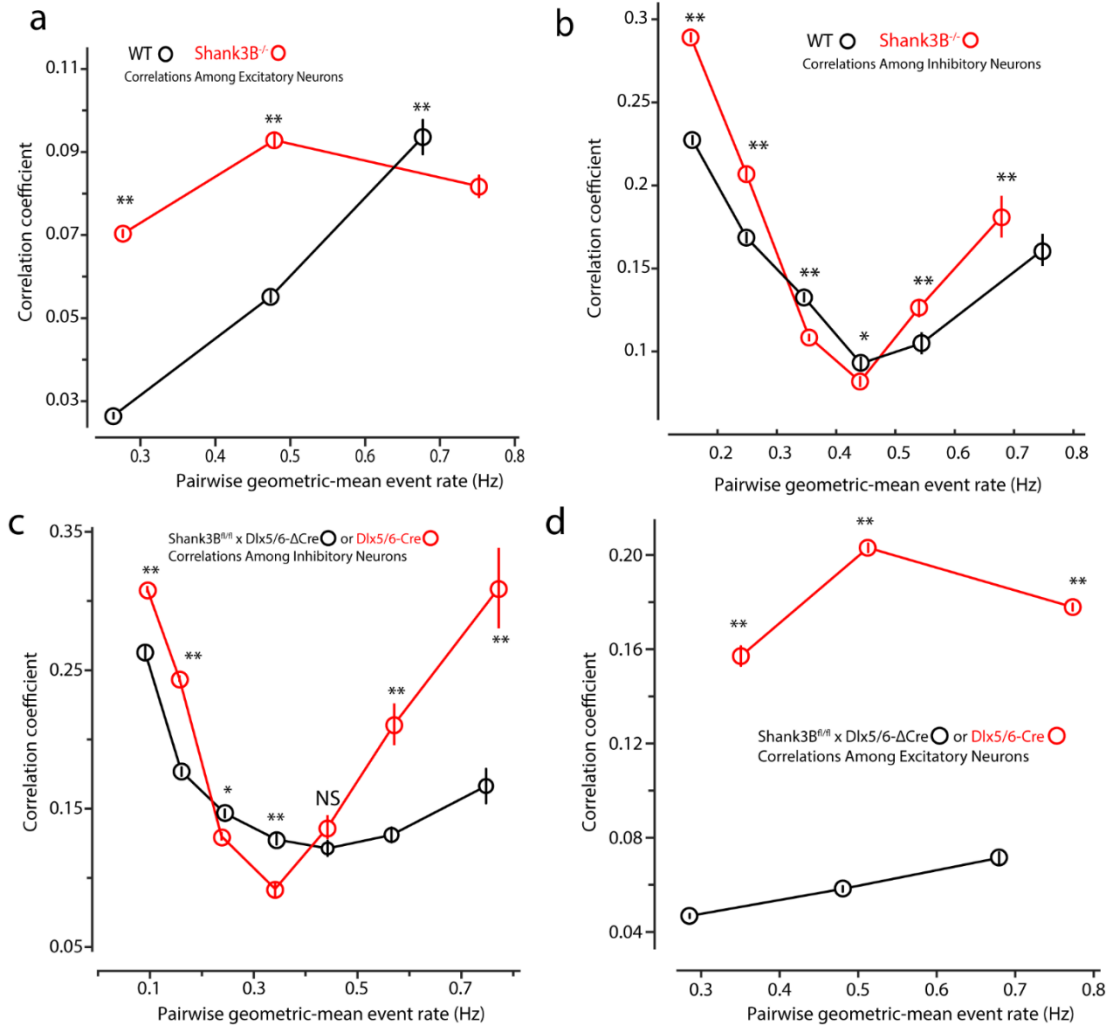
Supplementary Figure 1. The Relationship Between Sensitivity and Criterion are the Same for WT and *Shank3B*^{-/-} Animals. (a) Signal detection diagram showing the standard definition of d' (sensitivity index) and 'criterion location' (crit.). Sensitivity describes the degree to which the animal's response probability for a stimulus (blue) differs from the response probability for no-stimulus trials (red). Criterion location is the inferred position that a reporter has placed their decision boundary. For this example, criterion is placed in the middle of the overlapping region, which is the region that this animal would be uncertain is noise or signal. A 'rational' reporter would place their criterion here as they would get half of the uncertain trials right and half wrong. (b) An illustration of the two ways a reporter could show improved detection performance, compare each to a. Left, the reporter has a more separated signal representation, relative to the noise (true d' increase). Right, the animal can shift their criterion to be more impulsive. Here, the criterion moves towards the center of the noise distribution, so the animal will false report more often, but they will get more of the uncertain stimuli right. (c) A plot of criterion location vs. d' for all WT animals (black dots) and *Shank3B*^{-/-} animal's (red dots) sessions. This relationship was well described by a simple linear fit ($p=0.003$ WT, $p=0.001$ *Shank3B*^{-/-}; linear regression F-Test, $n=110$ total sessions per group, comprising 11 sessions per mouse, and 10 mice for both WT and *Shank3B*^{-/-} groups) and there was no significant differences in the correlation coefficients (Spearman ρ) between d' and criterion computed for each session and compared between each genotype ($p=0.7$, two-tailed bootstrap mean-difference test, $n=110$ correlation coefficients for both WT and *Shank3B*^{-/-} groups, comprising 11 sessions per mouse, and 10 mice per group).

Supplementary Figure 2



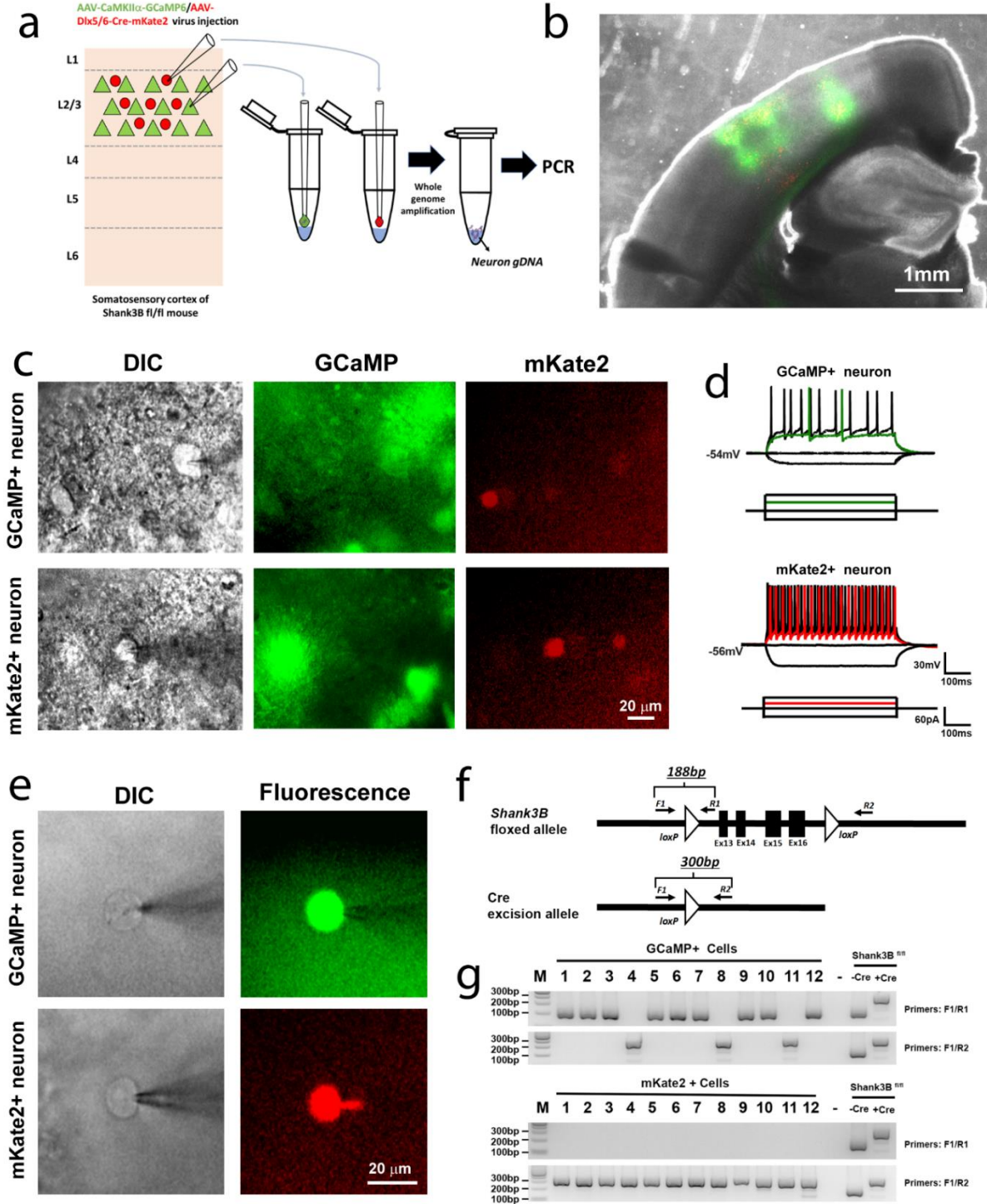
Supplementary Figure 2. Hit Rate and False Alarm Rate for Behaviorally-Trained WT and *Shank3B*^{-/-} Mice. Fifteen WT and seventeen *Shank3B*^{-/-} mice were trained to perform detection. Trials without pre-stimulus licking were pooled across all behavioral sessions in which mice performed at least 50 trials. We took all of the trials/sessions that overlapped for all mice in our sample. This included data from just as the mice were beginning to show proficiency in the task ($d' \geq 1$) to when performance stabilized. **(a)** The hit and false-alarm rates were computed in 50-trial wide bins. Hit rate estimates are shown for all stimuli, regardless of amplitude. Solid lines represent the mean and the shaded regions around the lines represent the standard error of the mean. **(b)** Same as a, but hit-rates were estimated for strong and weak stimuli separately. The shaded region in blue denotes when performance stabilized and the trials used for further analysis.

Supplementary Figure 3



Supplementary Figure 3. Relationships between spontaneous pairwise event rate and correlation for sample groups. (a). We pooled the geometric mean and correlation coefficients (Spearman ρ) for all possible neuronal pairs in imaging sessions of spontaneous firing of excitatory neurons in WT (black, $n=6$ mice) and *Shank3B*^{-/-} mice (red, $n=6$ mice). These data are the same as those in Fig. 2c. (** $p < 0.0001$, bootstrap mean-difference test). We plotted each pair's correlation coefficient (Spearman ρ) against the pair's mean event rate, then we computed the average rate and correlation coefficient for three event rate bins. (b) Same as a, but for inhibitory neurons imaged in *Shank3B*^{-/-} (red) and WT (black) mice, as presented in Fig. 3c. (* $p < 0.05$, and ** $p < 0.0001$, bootstrap mean-difference test, p -values in order from left-to-right: < 0.0001 , < 0.0001 , < 0.0001 , 0.001 , < 0.0001 , < 0.0001). (c) Same as a-b, but for inhibitory neurons imaged in *Shank3B*^{fl/fl} mice injected in vS1 with either *Dlx5/6-ΔCre* (black) or *Dlx5/6-Cre* (red). The data here corresponds with that in Fig. 4c (* $p < 0.05$, ** $p < 0.0001$, and NS $p > 0.05$, bootstrap mean-difference test, p -values in order from left-to-right: < 0.0001 , < 0.0001 , 0.002 , < 0.0001 , 0.8 , < 0.0001 , < 0.0001). (d) Same as a-c, but for excitatory neurons imaged in *Shank3B*^{fl/fl} mice injected in vS1 with either *Dlx5/6-ΔCre* (black) or *Dlx5/6-Cre* (red). The data here corresponds with that in Fig. 5d. Asterisks denote significant differences (** $p < 0.0001$, bootstrap mean-difference test). All Bootstrap mean-difference tests were two-sided. For all plots, the center of the circles represents the mean and the error bars represent to the standard error of the mean.

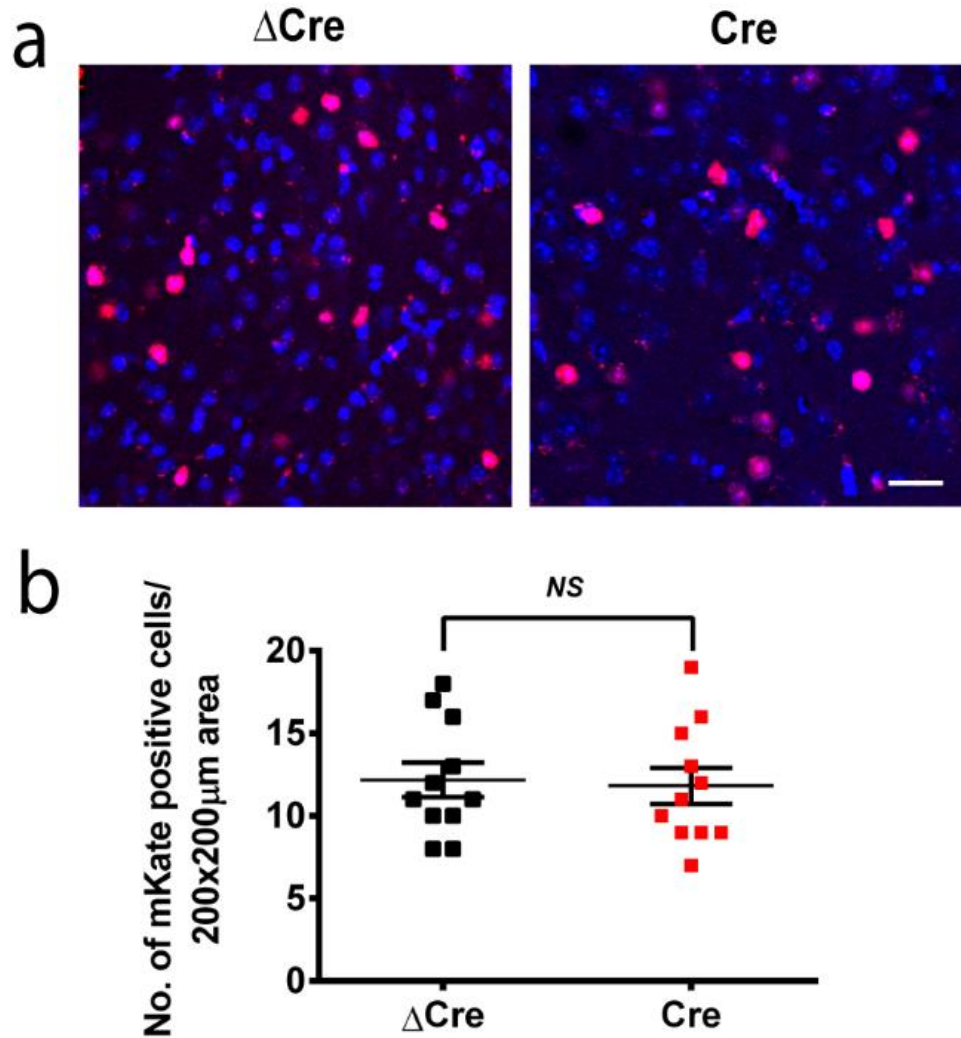
Supplementary Figure 4



Supplementary Figure 4. Single-cell PCR of *Shank3* Deletion in Interneurons and Excitatory Neurons from the Acute Brain Slices of AAV-Dlx5/6-Cre-mKate2 and AAV-CaMKII-GCaMP6 injected *Shank3B^{fl/fl}* Mice. (a) Experimental design for single-cell PCR process. (b) The overlay of

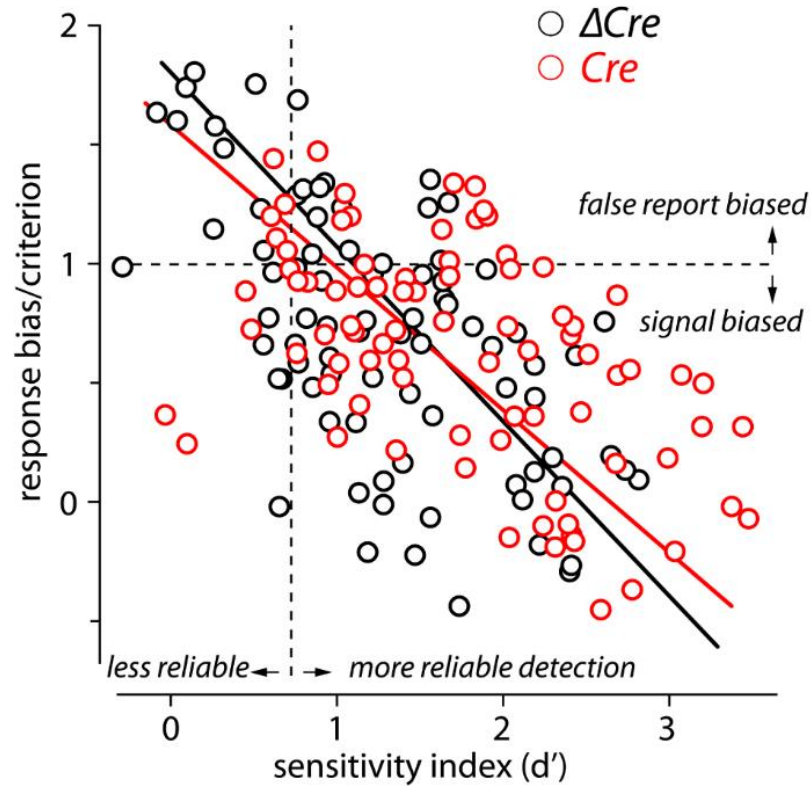
differential interference contrast (DIC) and fluorescent images from an acute brain slice of AAV-Dlx5/6-Cre-mKate2 and AAV-CaMKII-GCaMP6 injected *Shank3B^{fl/fl}* mouse. Red is the expression of Cre-mKate2 and green is the expression of GCaMP6. **(c)** DIC and fluorescent images of a GCaMP⁺ neuron (excitatory neuron, upper row) and a mKate2⁺ neuron (interneuron, bottom row) in patch-clamp configuration. **(d)** Example traces of membrane voltage changes for a GCaMP⁺ (top) and mKate2⁺ (bottom) neurons in response to step current injection in current clamp mode. **(e)** Representative DIC and fluorescent images of the picked-up neurons for single cell genotyping. **(f)** The location of primers for single cell genotyping in the *Shank3B* floxed (upper panel) and Cre excised (bottom panel) genome in the *Shank3B^{fl/fl}* mice. **(g)** The representative single cell PCR results from 12 GCaMP⁺ (upper panel) and mKate2⁺ neurons (bottom panel). M is 1Kb+ DNA ladder. “-” is the negative control (PCR reaction without DNA sample). “-Cre” is the cell from *Shank3B^{fl/fl}* without Cre expression. “+Cre” is the cell from *Shank3B^{fl/fl}* with Cre expression. The data in **(b-c)** was from 42 excitatory neurons (AAV-CaMKII-GCaMP6 positive neurons) and 33 inhibitory neurons (AAV-Dlx5/6-Cre-mKate2 positive neurons) in three AAV-Dlx5/6-Cre-mKate2 and AAV-CaMKII-GCaMP6 injected *Shank3B^{fl/fl}* mice. Single-cell PCR was performed 3 independent times.

Supplementary Figure 5



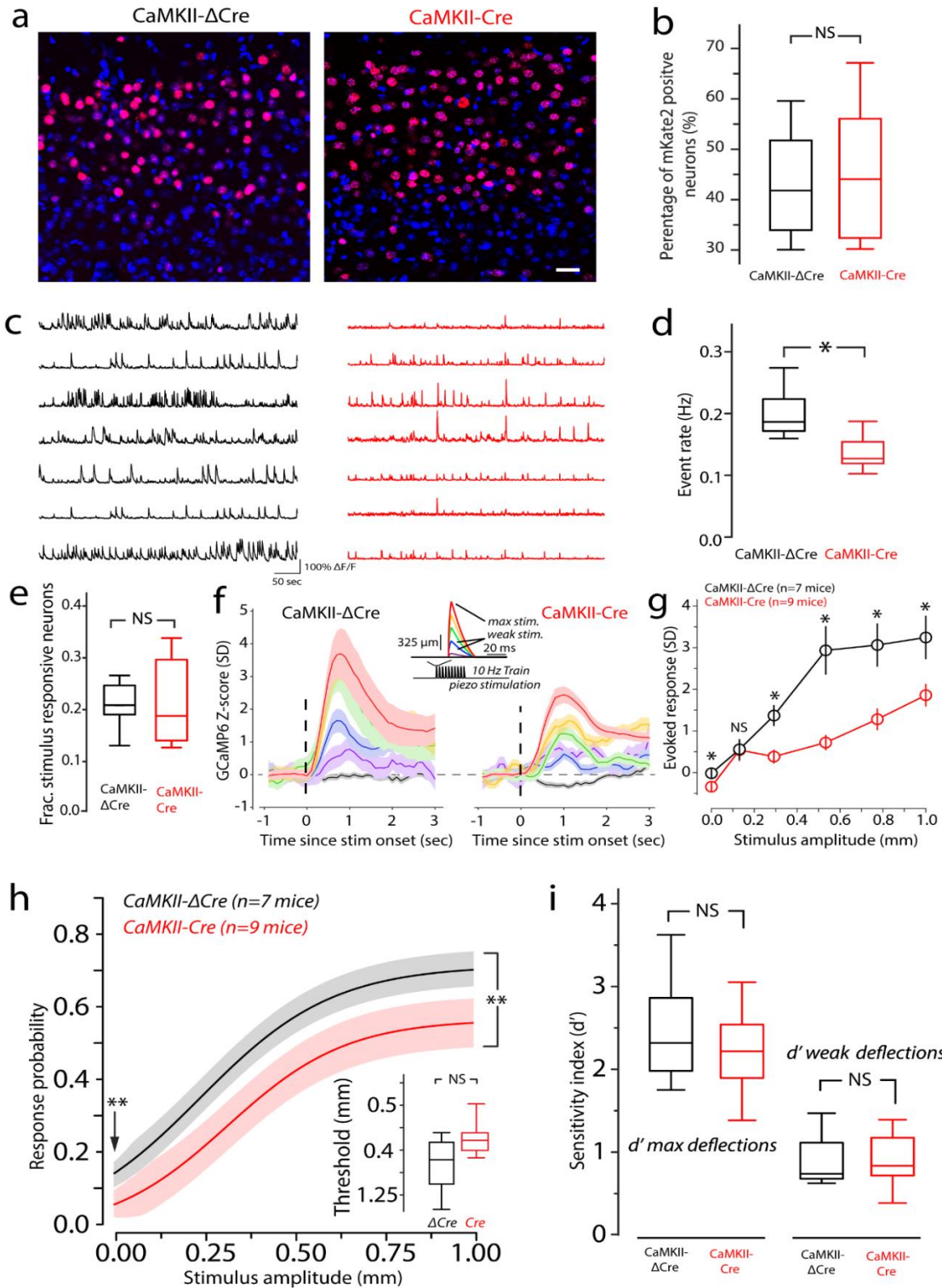
Supplementary Figure 5. Expression of AAV-Dlx5/6- Δ Cre-mKate2 and AAV-Dlx5/6-Cre-mKate2 in Somatosensory Cortex of *Shank3B^{fl/fl}* Mice. (a) Confocal images showing the expression of AAV-Dlx5/6- Δ Cre-mKate2 (left) or AAV-Dlx5/6-Cre-mKate2 (right) virus and DAPI staining in the somatosensory cortex layer II-III of the *Shank3B^{fl/fl}* mice (blue: DAPI; red: AAV-Dlx5/6- Δ Cre-mKate2 or AAV-Dlx5/6-Cre-mKate2), Scale bar is 50 μ m. (b) Quantification of mKate2 positive cells in somatosensory cortex layer II-II between mice injected with AAV-Dlx5/6- Δ Cre-mKate2 or AAV-Dlx5/6-Cre-mKate2 virus (n=11 slices from two mice injected with AAV-Dlx5/6- Δ Cre-mKate2 virus, n=11 slices from two mice injected with AAV-Dlx5/6-Cre-mKate2 virus). Data are presented as mean \pm s.e.m. NS denotes no difference. $p = 0.8$, two-tailed unpaired Student's t -test, $t = 0.24$, Degrees of freedom = 20. Δ Cre: AAV-Dlx5/6- Δ Cre-mKate2-injected mouse group; Cre: AAV-Dlx5/6-Cre-mKate2-injected mouse group.

Supplementary Figure 6



Supplementary Figure 6. The Relationship Between Sensitivity and Criterion are the Same for AAV-Dlx5/6- ΔCre and AAV-Dlx5/6-Cre Injected *Shank3B^{fl/fl}* Mice. This is the same plot made in Supplementary Figure 1c, but for Dlx5/6- ΔCre (control animals) and Dlx5/6-Cre-injected animals (S1 localized interneuron *Shank3B* knockout). Criterion is plotted as a function of apparent sensitivity (d') for all sessions and stimuli, regardless of strength (n=84 sessions; 14 consecutive sessions from each mouse; n=6 mice from each group). Red denotes Dlx5/6-Cre animals and black denotes Dlx5/6- ΔCre animals. Lines are best linear fit. The correlation coefficients (Spearman ρ) for each genotype were not significantly different ($p=0.4$; tail-probability). ΔCre : AAV-Dlx5/6- ΔCre -mKate2-injected mouse group; Cre: AAV-Dlx5/6-Cre-mKate2-injected mouse group.

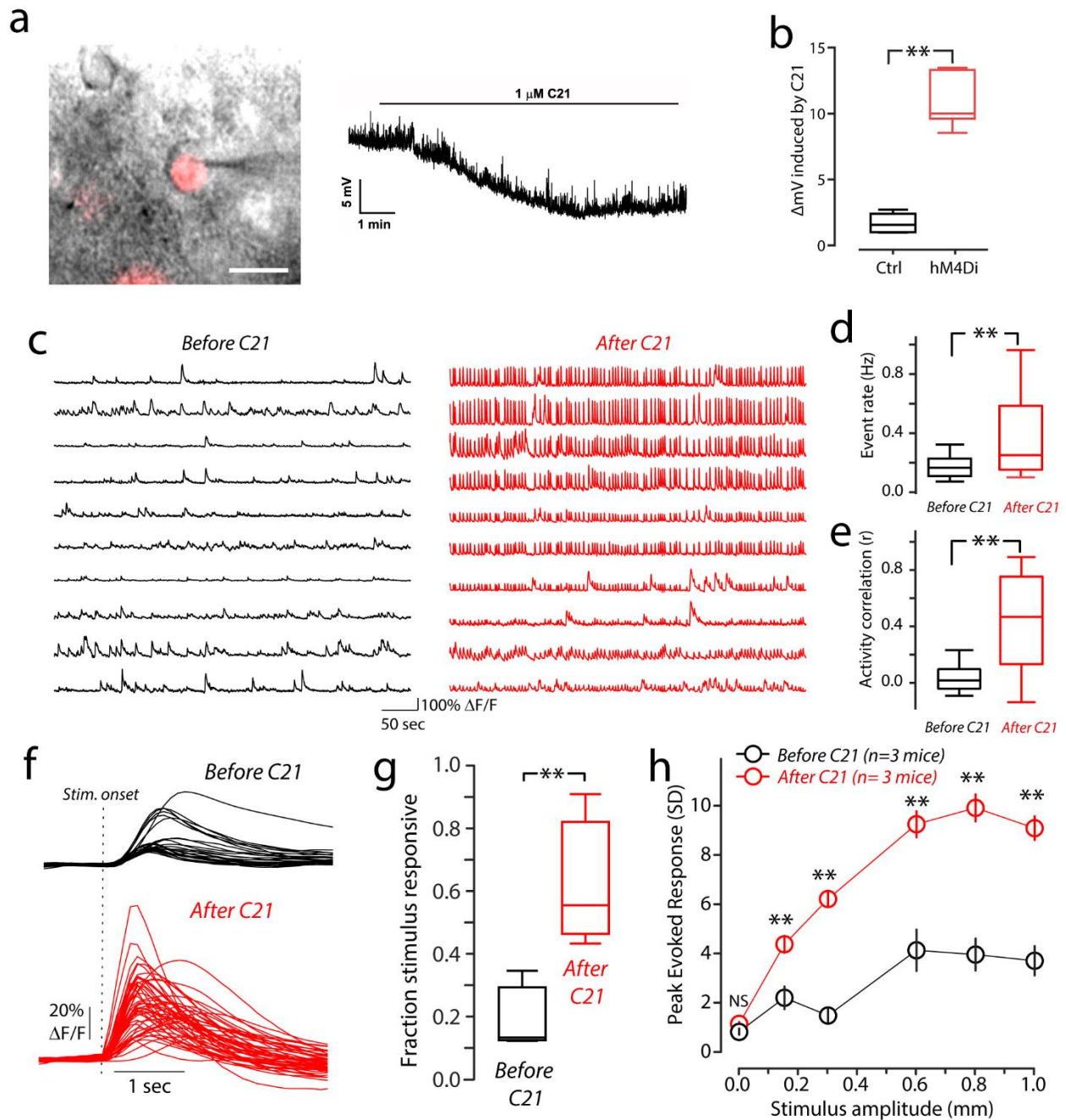
Supplementary Figure 7



Supplementary Figure 7. Selective-Deletion of *Shank3B* in Excitatory Neurons Leads to Neuronal Hypoactivity and Stimulus Hypo-Reactivity. (a) Confocal images showing the expression of AAV-CaMKII- Δ Cre-mKate2 (left) or AAV-CaMKII-Cre-mKate2 (right) virus and

DAPI staining in the somatosensory cortex layer II-III of the *Shank3B^{fl/fl}* mice (blue: DAPI; red: AAV-CaMKII- Δ Cre-mKate2 or AAV-CaMKII-Cre-mKate2). Scale bar is 50 μ m. **(b)** Box-plot showing the quantification of mKate2 positive cells in somatosensory cortex layer II-II between *Shank3B^{fl/fl}* mice injected with AAV-CaMKII- Δ Cre-mKate2 (mean \pm s.e.m.: 41.8 ± 3.2) or AAV-CaMKII-Cre-mKate2 virus (mean \pm s.e.m.: $44.1 \pm 4.1\%$, $p=0.8$, $n=12$ slices from 4 mice in each group, two-tailed unpaired Student's t -test, $t=0.42$, Degrees of freedom = 22). **(c)** Example spontaneous $\Delta F/F$ time-series traces from a CaMKII- Δ Cre (left; black) and CaMKII-Cre (right; red) injected *Shank3B^{fl/fl}* mouse. **(d)** Box-plots quantifying differences of spontaneous calcium event rate that was determined by counting the total number of deconvolved individual Ca^{2+} -events for ten minutes ($n=561$ neurons from 7 CaMKII- Δ Cre-injected; $n=696$ neurons from 9 CaMKII-Cre-injected mice). Asterisk denotes a statistically-significant difference between the sample groups ($*p=0.0002$; bootstrap mean-difference test). **(e)** Box-plots showing the fraction of neurons determined to be stimulus responsive neurons in CaMKII- Δ Cre (black; $n=7$ mice) and CaMKII-Cre groups (red; $n=9$ mice; NS denotes no difference, $p=0.1$, bootstrap mean-difference test). **(f)** Left panel: The magnitude of evoked responses in Δ Cre-injected *Shank3B^{fl/fl}* mice, across the range of stimulus amplitudes. We quantified this by constructing peri-stimulus time histograms (PSTHs) from Z-scored evoked-responses for all of the responsive neurons. The average response for each stimulus amplitude is color coded as indicated by the inset showing the piezo-stimulus waveform (red is the maximal deflection, purple is the weakest). Lines on all plots indicate the mean and the shaded regions corresponds to the standard error of the mean. Right panel: same as in left panel, but from Cre-injected *Shank3B^{fl/fl}* mice. **(g)** Comparison of peak-evoked responses across the stimulus-amplitudes tested for responsive neurons in CaMKII- Δ Cre (black; $n=107$ neurons from 7 mice) and CaMKII-Cre groups (red; $n=150$ neurons from 9 mice). The center of the circles represents the mean and the error bars represent to the standard error of the mean. Asterisks denote statistically significant differences ($*p<0.05$, NS denotes no difference $p>0.05$; bootstrap mean-difference test, p -values in order from left-to-right: 0.02, 0.4, 0.0001, 0.0004, 0.003, and 0.02). **(h)** Mean psychometric curves (non-normalized sigmoidal function fits) from CaMKII- Δ Cre (black; $n=7$ mice) and CaMKII-Cre groups (red; $n=9$ mice). Solid lines denote the mean, and the shaded regions are the standard error of the mean. Asterisks next to the curves denote a significant-difference in the total curve quantified by testing the differences in peak performance, and false-alarm rate ($**p<0.0001$; bootstrap mean-difference test). The inset show a non-significant difference of detection threshold between groups ($p=0.07$; bootstrap mean-difference test, CaMKII- Δ Cre threshold mean \pm s.e.m.: $328 \pm 100 \mu$ m, $n=7$; CaMKII-Cre: $496 \pm 44 \mu$ m, $n=9$). In addition, there was no difference in the unitless slope-factor between CaMKII-Cre and CaMKII- Δ Cre groups (CaMKII- Δ Cre mean \pm s.e.m.: 191 ± 41 ; CaMKII-Cre: 247 ± 27 ; $p=0.2$, bootstrap mean-difference test). **(i)** Left, Box and whisker plots showing the bootstrap estimate of population mean d' for maximal stimuli for CaMKII- Δ Cre (black; $n=7$) and CaMKII-Cre (red; $n=9$) groups from the same sessions used in **h**. Right, same but showing d' for weak stimuli. There was a non-significant difference in both maximal d' ($p=0.3$) and weak d' ($p=0.9$; bootstrap mean-difference test). Box-and-whisker plots show median values (middle vertical bar) and 25th (bottom side of the box) and 75th percentiles (top side of the box) with whiskers indicating the range. All bootstrap mean-difference tests were two-sided. CaMKII- Δ Cre: AAV-CaMKII- Δ Cre-mKate2-injected mouse group; Cre: AAV-CaMKII-Cre-mKate2-injected mouse group.

Supplementary Figure 8



Supplementary Figure 8. Chemogenetic Downregulation of Inhibitory Neuronal Activity Drives Excitatory Neuronal Hyperactivity. (a) Left panel: The overlay of DIC and fluorescence image showing the recording from a neuron infected with AAV encoding hM4Di-rls-tdTomato. Right: Representative trace of the same neuron recorded in the right panel were exposed to C21 (1 μ M). Scale bar is 20 μ m. (b) Box-plots of mean voltage changes for control (black, n = 4 mKate2 negative cells) and hM4Di-expressed neurons (red, n=5 mKate2 positive cells) after C21 treatment

(** $p < 0.0001$; bootstrap mean-difference test). (c) Example CaMKII-GCaMP6 spontaneous $\Delta F/F$ time-series traces of an AAV-Dlx5/6- hM4Di-injected mouse before (black) and after (red) C21 treatment. (d) Box-plots quantifying differences of spontaneous calcium event rate that was determined by counting the total number of deconvolved individual Ca^{2+} -events for ten minutes (n=258 neurons before C21 treatment from 3 mice; 269 neurons after C21 treatment from 3 mice). Asterisk denotes a statistically-significant difference between the sample groups (** $p < 0.0001$; bootstrap mean-difference test). (e) Box-plots quantifying differences of correlation coefficients (n=12,860 pairs before C21 treatment from 3 mice; n=13,378 pairs after C21 treatment from 3 mice) Asterisk denotes a statistically-significant difference between the sample groups (** $p < 0.0001$; bootstrap mean-difference test). (f) Example traces showing the $\Delta F/F$ responses to maximal (1mm) whisker deflections stimulus of the responsive neurons before (black, n=46 neurons from 3 mice) and after C21 treatment (red, n=119 neurons from 3 mice). The dashed line indicates the onset of the whisker stimulus. (g) Box-plots showing the fraction of neurons determined to be stimulus responsive before (black, n= 3 mice) and after C21 treatment (red, n=3 mice). Asterisk denotes a statistically-significant difference between the sample groups (** $p < 0.0001$; bootstrap mean-difference test). (h) Comparison of peak-evoked responses across the stimulus-amplitudes tested before (black) and after (red) C21 treatment. Asterisks denote statistically significant differences (black: before C21 treatment, n=46 neurons from 3 mice, red: after C21 treatment, n=119 neurons from 3 mice; ** $p < 0.0001$, * $p < 0.05$, and NS $p > 0.05$; p -values in order from left-to-right: 0.2, < 0.0001 , < 0.0001 , < 0.0001 , < 0.0001 , < 0.0001); bootstrap mean-difference test). Box-and-whisker plots show median values (middle vertical bar) and 25th (bottom side of the box) and 75th percentiles (top side of the box) with whiskers indicating the range. All bootstrap mean-difference tests were two-sided.